ON THE VISCOSITY AND PHYSICAL ORIGIN OF STABILITY OF WEAKLY BOUND COMPLEXES CdZn, HgZn AND HgCd

Michal ILČIN[1], Vladimír LUKEŠ[2], Viliam LAURINC[3,*] and Stanislav BISKUPIČ[4]

Institute of Physical Chemistry and Chemical Physics, Slovak University of Technology, Radlinského 9, SK-812 37 Bratislava, Slovak Republic; e-mail: [1] michal.ilcin@stuba.sk, [2] vladimir.lukes@stuba.sk, [3] viliam.laurinc@stuba.sk, [4] stanislav.biskupic@stuba.sk

Received October 16, 2006
Accepted January 23, 2007

Dedicated to Professor Vladimír Kvasnička on the occasion of his 65th birthday.

Supermolecular CCSD(T) *ab initio* calculations of potential energy curves for the electronic ground states of heteronuclear van der Waals complexes formed from the atoms of IIB group are presented. The physical origin of stability of the studied structures was analyzed by the symmetry-adapted perturbation theory. The magnitude of dispersion term increases with the increase of diatomic mass, but the relative importance of dispersion vs Hartree–Fock induction energies decreases in the order CdZn > HgZn > HgCd. Theoretical calculations of the temperature dependence of the shear viscosity for low-density binary mixtures are in good agreement with the temperature dependences of the shear viscosity obtained from empirical formula.

Keywords: *Ab initio* calculations; Potential energy curves; van der Waals complexes; Shear viscosity; Zinc; Cadmium; Mercury; Quantum chemistry.

The interest in the weakly bound complexes formed from the atoms of the IIB group has been revived in recent years mainly because of their prospective role in excimer lasers and catalytic and adsorption processes on various surfaces[1,2]. Several experimental studies of excitation and fluorescence spectra of the HgZn excimer were investigated using the pump-and-probe method of laser spectroscopy[3]. Other available experimental data are low-density shear viscosity measurements of pure IIB group substances[4]. Based on these measurements and on the results of dimeric spectroscopy, the ground-state equilibrium distances r_e were determined as 3.71 Å for Hg_2, 4.38 Å for Cd_2 and 4.68 Å for Zn_2 (ref.[5]). These distances are larger by ca. 10% for Zn and by ca. 6% for Cd than the previous experimental values obtained from the free-jet-beam-expansion and laser-excitation techniques[6]. The IIB group diatomic complexes have been studied also theoretically[7–15].

Collect. Czech. Chem. Commun. 2007, Vol. 72, No. 3, pp. 363–378

doi:10.1135/cccc20070363

In these works the potential energy curves of ground and excited states calculated at different levels of theory are provided. Besides potential energy curves the material properties (e.g. spectroscopic constants, polarizabilities, second virial coefficients) can be found in these works.

In our recent work[16] we have also theoretically studied the homonuclear IIB group dimers. The calculated potential energy curves were used for calculations of temperature dependences of shear viscosity and these were compared to the experimental data. The largest deviations from experimental data were observed in the case of the zinc dimer (see Fig. 3 in ref.[16]).

The heteronuclear IIB group complexes have not been studied theoretically so exhaustively as the homonuclear ones. Of previous theoretical studies one can mention the multireference CI study of Czuchaj et al. for CdHg (ref.[17]) and for ZnHg and ZnCd systems[18] and MRCI study of potential energy curve for HgZn of Gao et al.[19], or the perturbational (MP2–MP4) and QCISD(T) study of Bieroń and Baylis[9,20]. Of experimental studies, the laser spectroscopy studies of HgCd (ref.[21]) and HgZn (ref.[22]) system should be mentioned. There are quite large deviations in the ground-state equilibrium internuclear distances and well depths between different theoretical and experimental approaches (see Table 1 in ref.[9]).

Despite the above mentioned supermolecular (SM) *ab initio* calculations on the group IIB dimers and heteroatomic complexes, there is still a demand for the detailed analysis of interaction energy contributions which stabilise the above mentioned systems. Encouraged by earlier theoretical studies, one of the goals of this work was to provide a basis-set-superposition-error (BSSE)-free characterization of heteronuclear IIB group diatomic complexes at the supermolecular CCSD(T) theoretical level. For the calculations we decided to use the pseudopotentials extended with a set of mid-bond functions. The same basis sets were used in our previous study of homonuclear IIB group dimers[16]. The physical origin of the van der Waals (vdW) structure stability was analyzed using the symmetry-adapted perturbation theory[23] (SAPT).

The second goal of our study was utilization of the relation between the microscopic vdW interaction potential and macroscopic transport properties. From the obtained theoretical potential energy curves and from the potential energy curves of homonuclear IIB group complexes published recently by us in ref.[16], temperature dependences of shear viscosity were simulated. The calculations of shear viscosity were performed using a rigorous, kinetic theory based approach as well as empirical formulae commonly used in the technical practice.

THEORETICAL

Quantum Chemical Calculations

Ab initio studies were evaluated using the supermolecular (SM) approach[24] where the interaction energy is obtained as the difference between the value of the energy of the complex E_{AB} and the sum of the energies of its constituents ($E_A + E_B$)

$$\Delta E = E_{AB} - E_A - E_B \qquad (1)$$

where symbol Δ denotes terms calculated as differences.

The energies can be calculated at various levels of theory, at the Hartree–Fock (HF) level or at theoretical level involving correlation energy, e.g. the Møller–Plesset (MP) level[25] or the more popular coupled cluster (CC) level[26]. Although the SM approach is conceptually and computationally simple, it does not offer a detailed picture of interaction forces. On the other hand, the intermolecular perturbation[24] theory (I-PT) allows direct calculations of electrostatic (E_{elst}), exchange-penetration (E_{exch}), dispersion (E_{disp}) and induction (E_{ind}) contributions which provide physical interpretation of the interactions between the monomers of a complex

$$E_{int} = \sum E_{els}^{(nij)} + \sum E_{ind}^{(nij)} + \sum E_{disp}^{(nij)} + \sum E_{exch}^{(nij)} + \sum E_{other}^{(nij)} . \qquad (2)$$

The superscript *n* in Eq. (*2*) denotes the order of the perturbation V_{AB} and *i* (*j*) indicate the order of the Møller–Plesset fluctuation potential for the A (B) system. Last term $\sum E_{other}^{(nij)}$ denotes all mixed terms and higher order terms with not so simple physical interpretation[24].

The HF-SCF interaction energy can be decomposed as follows

$$\Delta E^{HF} = \Delta E^{HL} + \Delta E_{def}^{HF} \qquad (3)$$

where ΔE^{HL} is the Heitler–London (HL) energy[27] and ΔE_{def}^{HF} is the HF deformation contribution[24]. According to the I-PT defined in the orthogonalized basis sets[28,29], ΔE^{HL} may be further divided into the first-order Hartree–Fock electrostatic ($E_{els}^{(100)}$, for notation for this and other perturbation terms, see, e.g., ref.[23]) and HL exchange-penetration ΔE_{exch}^{HL} components

$$\Delta E^{\mathrm{HL}} = \Delta E^{\mathrm{HL}}_{\mathrm{exch}} + E^{(100)}_{\mathrm{els}} . \qquad (4)$$

The HF deformation energy originates in the mutual electric polarization effects. This term might be approximated using the sum of the following two perturbation terms: $E^{(200)}_{\mathrm{ind}}$ and $E^{(200)}_{\mathrm{exch\text{-}ind}}$ (second-order HF Coulomb and exchange induction energies)[23].

The second-order MP2 correlation interaction energy can be partitioned as

$$\Delta E^{(2)}_{\mathrm{int}} = E^{(12)}_{\mathrm{els}} + E^{(200)}_{\mathrm{disp}} + E^{(200)}_{\mathrm{exch\text{-}disp}} + \Delta E^{(2)}_{\mathrm{other}} \qquad (5)$$

where $E^{(12)}_{\mathrm{els}}$ denotes the second-order electrostatic correlation energy (containing $E^{(102)}_{\mathrm{els}}$ and $E^{(120)}_{\mathrm{els}}$ energies). $E^{(200)}_{\mathrm{disp}}$ and $E^{(200)}_{\mathrm{exch\text{-}disp}}$ represent the second-order Hartree–Fock dispersion[30] and exchange-dispersion energies[23]. $\Delta E^{(2)}_{\mathrm{other}}$ encompasses the remaining exchange and deformation correlation corrections as well as the response effects, not included in the first three second order terms of SAPT.

Using the diagrammatic techniques, it is possible to distinguish the third-order interaction energy contributions like the dispersion-correlation ($E^{(210)}_{\mathrm{disp}}$, $E^{(201)}_{\mathrm{disp}}$) and Hartree–Fock third-order dispersion ($E^{(300)}_{\mathrm{disp}}$) energies[29]. However, complete physical interpretation of higher than second-order contributions of the interaction electron-correlation energies is not straightforward.

Shear Viscosity Calculations

At low density, the shear viscosity η of one-component real gas can be written as[31,32]

$$h = \frac{5}{16} \frac{(m\pi k_B T)^{1/2}}{\pi\sigma^2 \Omega^{(2,2)^*}(T^*)} \qquad (6)$$

where m is the atomic weight, k_{B} is the Boltzmann constant, σ is the collision diameter for low energy collisions (it is the value of r for which the potential function is equal to zero), T is the absolute temperature and T^* is the reduced temperature ($T^* = k_{\mathrm{B}}T/D_{\mathrm{e}}$, where D_{e} is the well depth of potential energy curve). The expression for the shear viscosity (*6*) has the same form as in the rigid-sphere model except for the term $\Omega^{(2,2)^*}(T^*)$ in the denominator. The transport coefficients of low-density real gas can be expressed in the terms of the collision integrals $\Omega^{(l,s)}$. These are divided by corresponding

rigid-sphere values of $\Omega^{(l,s)}$ for obtaining the expressions for transport coefficients in a form similar to the rigid-sphere model with a specific factor describing the deviation from this model. This leads to the reduced collision integrals $\Omega^{(l,s)*}(T^*)$ which can be defined as[32]

$$\Omega^{(l,s)*}(T^*) = \frac{1}{(s+1)!\,T^{*\,s+2}} \int_0^\infty \mathrm{e}^{-\frac{E^*}{T^*}} E^{*\,s+1} Q^{(l)*}(E^*)\,\mathrm{d}E^* \qquad (7)$$

where E^* is reduced kinetic energy ($E^* = E/D_e$) and $Q^{(l)*}$ are reduced cross-sections as they are defined in ref.[32] in terms of reduced parameters.

Analogously to the one-component gas, one can calculate the viscosity η_{12} from the potential function $V_{12}(r_{12})$ of the interaction of two different atoms characterized by the collision diameter σ_{12} and the dissociation energy $D_{e,12}$. Viscosity η_{12} is given by

$$\eta_{12} = \frac{5}{16} \frac{\left(\frac{2m_1 m_2}{m_1 + m_2} \pi k_B T \right)^{1/2}}{\pi \sigma_{12}^2 \Omega_{12}^{(2,2)*}(T^*)} \qquad (8)$$

where m_1, m_2 are the atomic weights of the atoms 1, 2 and $\Omega_{12}^{(2,2)*}(T^*)$ is the collision integral for the potential function $V_{12}(r_{12})$. It can be evaluated according to Eq. (*7*) with reduced parameters calculated using the heteronuclear potential parameters σ_{12} and $D_{e,12}$.

In a mixture of two components, collisions occur between the atoms 1 and 1, between the atoms 2 and 2 and between the atoms 1 and 2. The viscosity η_{12} represents therefore only one of the three contributions to viscosity of the binary mixture. One should mention the close relationship between this viscosity and the coefficient of diffusion D_{12} (ref.[32])

$$\eta_{12} = \frac{5}{3} \frac{M_1 M_2}{(M_1 + M_2)} \frac{pD_{12}}{A_{12}^* RT} \qquad (9)$$

where p is pressure, M_1, M_2 are molar weights of components and A_{12}^* is defined as

$$A_{12}^* = \frac{\Omega_{12}^{(2,2)*}(T^*)}{\Omega_{12}^{(1,1)*}(T^*)} \,. \qquad (10)$$

This relationship allows to check the calculated η_{12} through the measured diffusion coefficient D_{12}. For the viscosity of a binary mixture the following expression can be written[32]

$$\eta_{\mathrm{mix}} = \frac{1 + Z_\eta}{X_\eta + Y_\eta} \tag{11}$$

where

$$X_\eta = \frac{x_1^2}{\eta_1} + \frac{2x_1x_2}{\eta_{12}} + \frac{x_2^2}{\eta_2} \tag{12}$$

$$Y_\eta = \frac{3}{5} A_{12}^* \left\{ \frac{x_1^2}{\eta_1} \frac{M_1}{M_2} + \frac{2x_1x_2}{\eta_{12}} \frac{(M_1 + M_2)^2}{4M_1M_2} \frac{(\eta_{12})^2}{\eta_1\eta_2} + \frac{x_2^2}{\eta_2} \frac{M_2}{M_1} \right\} \tag{13}$$

$$Z_\eta = \frac{3}{5} A_{12}^* \left\{ x_1^2 \frac{M_1}{M_2} + 2x_1x_2 \left[\frac{(M_1 + M_2)^2}{4M_1M_2} \left(\frac{\eta_{12}}{\eta_1} + \frac{\eta_{12}}{\eta_2} \right) - 1 \right] + x_2^2 \frac{M_2}{M_1} \right\} \tag{14}$$

with η_i, x_i representing the one-component viscosity and molar fraction of *i*-th component, respectively.

Calculation Details

All I-PT calculations were performed with SAPT program codes[23] interfaced to the Gaussian 03 program package[33]. Gaussian 03 was used for SM calculations as well. The supermolecular BSSE was determined by the counterpoise method of Boys and Bernardi[34]. The presented HF interaction energy terms were evaluated using the dimer-centered basis sets of the constituent monomers. In the present study the relativistic small core Stuttgart RSC 1997 ECP (hereafter ST97)[35] and CRENBL ECP (hereafter CRENBL)[36] pseudopotentials were used. In order to improve the effects of the basis set on the quality of interaction energy calculations the set of modified midbond functions [3s3p2d2f] of Tao and Pan (with the sp exponents: 0.9, 0.3, 0.1; d: 0.6, 0.2; f: 0.6, 0.2)[37] was used. These bond functions are fixed at the center of the axis defined by atoms.

The calculated dependences of interaction energies on the distances were fitted by the Morse potential function

$$V = D_e[\exp(-2\alpha(R - R_e)) - 2\exp(-\alpha(R - R_e))]\,. \qquad (15)$$

For calculation of the collision integral we use the computer code given in Appendix 12 of ref.[31] which is based on the method illustrated in ref.[38]. The accuracy of the numerical calculation is well within the second-order Chapman–Cowling correction[31].

Using the low-density shear viscosities of one-component IIB group element gases (see our previous work[16]) and η_{12} viscosities, one can calculate the low-density shear viscosity of a binary mixture of arbitrary composition. Shear viscosities were calculated according to the formulae (*7*)–(*14*). For the visualization purpose the following three mixture compositions were chosen: 25, 50 and 75 mole %.

We have not found in the literature the direct viscosity measurement data for binary mixtures of the IIB group elements in gaseous phase, but there are empirical formulae for the viscosity of binary gaseous mixtures[39]. These formulae are mostly based on weighting the viscosities of individual components, e.g.

$$\eta_{\mathrm{mix}} = \frac{\sum \eta_i x_i \sqrt{M_i}}{\sum x_i \sqrt{M_i}} \qquad (16)$$

or

$$\eta_{\mathrm{mix}} = \frac{\sum \eta_i x_i \sqrt{M_i T_{ci}}}{\sum x_i \sqrt{M_i T_{ci}}} \qquad (17)$$

where η_i, x_i, M_i and T_{ci} are the viscosity, mole fraction, molar weight and critical temperatures of the *i*-th component, respectively.

One of our goals was to assess the quality of these empirical formulae expressing the viscosity of mixtures. To be correct, the experimental viscosities of mixtures should be compared with those calculated according to the empirical formula using experimental viscosities of pure substances. Unfortunately, due to the lack of experimental data for binary mixtures such approach is impossible. A rigorous calculation of binary mixture viscosity can therefore serve as a benchmark for the assessment of the empirical formulae. For the consistency of the results, the same type of viscosity data of pure substances should be used in empirical and rigorous approaches. In contrast to the rigorous approach, in the empirical formula there is no term

originating from the mutual interaction of individual components like the viscosity η_{12} for which only theoretical data are available. So, we decided to use theoretical viscosity data for pure substances as well.

After assessment of the quality of the formulae (*16*) and (*17*) the better of them will serve for calculation of the binary mixture viscosity from experimental one-component gas viscosities. These viscosities will be considered as the experimental binary mixtures shear viscosities and will be used for evaluation of relative deviations of rigorous binary mixture shear viscosity calculations using CCSD(T)/ST97 potential energy curves. As the experimental one-component gas viscosities the Morse fits from Ceccherini and Moraldi work[5] will be used (dashed lines in Figs 1–3 in ref.[5]). In our previous work[16] the relative deviations of one-component gas viscosities (evaluated using CCSD(T)/ST97 potential energy curves) from experimental ones were:

for Zn –5.7% at 875 K and –6.7% at 950 K,
for Cd +4.3% at 800 K and +3.3% at 900 K and
for Hg +5.8% at 500 K and +0.5% at 900 K.

The calculations of all binary mixtures shear viscosities were performed in the temperature region 700–1000 K. The experimental viscosities were approximated with the following formulae:

$$\eta_{Zn}(T) \times 10^8 \text{ Pa s} = 6.10T + 753 \qquad (18)$$

$$\eta_{Cd}(T) \times 10^8 \text{ Pa s} = 7.01T + 336 \qquad (19)$$

$$\eta_{Hg}(T) \times 10^8 \text{ Pa s} = 10.05T - 462 \qquad (20)$$

where the temperature T is in K. The above defined relative deviations for 700 and 1000 K are, respectively: for Zn –3.9% and –7.4%, for Cd +4.8% and +2.0%, for Hg +3.3% and –1.0%.

RESULTS AND DISCUSSION

The calculated CCSD(T) spectroscopic constants of the metal dimers are compared in Table I with the theoretical and experimental results from other studies. One can notice a wide variability of the equilibrium interatomic distances in different theoretical and experimental studies. A considerable effect of mid-bond functions on the calculated equilibrium bond

lengths and dissociation energies should be noted. Without mid-bond functions the equilibrium bond lengths are much larger (using ST97 basis set by about 0.6–0.7 Å, using CRENBL basis set by about 1 Å in HgCd and 2 Å in systems containing Zn). The dissociation energies are underestimated more than twice (see Table I). In systems containing Zn using CRENBL basis set the results are completely unreliable (dissociation energies are 3 cm^{-1} for CdZn and 4 cm^{-1} for HgZn). CRENBL basis set provides much worse results than ST97. Mid-bond functions suppress the difference in the quality of CRENBL and ST97 basis sets.

TABLE I
Theoretical CCSD(T) and experimental spectroscopic properties of CdZn, HgZn and HgCd complexes. The values in parenthesis are obtained without mid-bond functions

System	Calculation	R_e, Å	ω_e, cm^{-1}	$\omega_e x_e$, cm^{-1}	D_e, cm^{-1}
CdZn	CRENBL	3.98 (6)	20.5	0.43	244 (3)
	ST97	3.94 (4.5)	20.8	0.44	246 (116)
	MP4/QCI[a]	4.50/4.55			257/237
	MRCI(SD)[b]	4.30			125
HgZn	CRENBL	3.87 (5.5)	19.7	0.36	269 (4)
	ST97	3.82 (4.5)	20.9	0.39	281 (117)
	MP4/QCI[a]	4.25/4.25			309/307
	MRCI(SD)[b]	3.44			370
	MRCI[c]	4.32	22.4	0.24	333
HgCd	Exp.[d]	4.66	19.3	0.3	310
	CRENBL	3.81 (4.8)	19.4	0.29	327 (72)
	ST97	3.81 (4.5)	19.5	0.27	355 (133)
	MP4/QCI[a]	4.15/4.15			345/334
	MRCI(SD)[e]	3.57			410
	Exp.[f]	3.95			335
	Exp.[g]	3.25			

[a] Ref.[9]; [b] ref.[18]; [c] ref.[19]; [d] ref.[22]; [e] ref.[17]; [f] semiempirical results of ref.[21]; [g] experimental value of ref.[40]

Using the I-PT decomposition, we analyzed the relative importance of fundamental components of the interaction energy at the stationary points of the potential energy curves. The relevance of electrostatic, induction and dispersion forces can be assessed on the basis of the relations of $E_{\mathrm{els}}^{(100)}$, $E_{\mathrm{ind\_resp}}^{(200)}$ and $E_{\mathrm{disp}}^{(200)}$ contributions (Figs 1 and 2). All separated SAPT contributions to the interaction energy calculated at the HF level of theory indicate

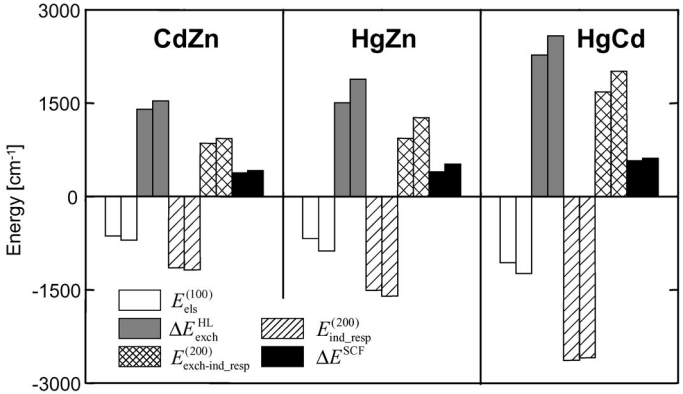

FIG. 1
Supermolecular SCF interaction energies and their relevant SAPT components for studied dimers. Each component is calculated in CRENBL (left bar) and ST97 (right bar) basis sets

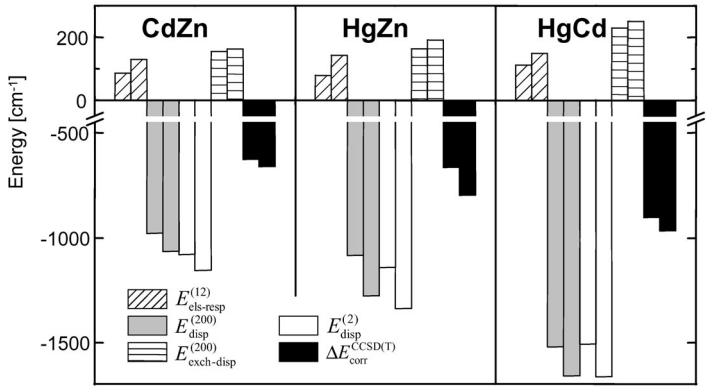

FIG. 2
Interaction correlation CCSD(T) energies and their relevant SAPT components for studied dimers. Each component is calculated in CRENBL (left bar) and ST97 (right bar) basis sets

an increase in absolute magnitudes with increasing reduced mass. The electrostatic induction energy $E^{(200)}_{ind\_resp}$ (the subscript resp indicates the inclusion of response effects, see e.g. ref.[24]) is larger than the pure HF electrostatic term $E^{(100)}_{els}$. However, the increase in the induction and electrostatic energies is different. The ratio $E^{(100)}_{els}$:$E^{(200)}_{ind\_resp}$ is maximal for CdZn and slightly decreases with increasing reduced mass, i.e. 0.59 (0.56) for CdZn, 0.55 (0.55) for HgZn and 0.48 (0.40) for HgCd in the ST97 (CRENBL) basis set. The induction energy $E^{(200)}_{ind\_resp}$ is composed of two contributions – energy of the induction interaction of atom 1 with the static field of atom 2 and vice versa. For the CdZn complex, these contributions are almost the same (–2.7 mE_h in ST97 and –2.6 mE_h in the CRENBL basis set). For HgZn and HgCd the ratio of the energy of the induction interaction of mercury atom with static field of zinc or cadmium atom to the energy of reverse induction interaction is 1.6 and 2.7–2.8 for ST97 and CRENBL basis set, respectively.

A dominant part of the interaction correlation energy naturally originates in the dispersion energy. Figure 2 shows the magnitude of the dispersion energy increasing in the order CdZn < HgZn < HgCd. On the other hand, the importance of dispersion vs induction interaction is decreasing in the order CdZn > HgZn > HgCd, which is demonstrated by the ratios $E^{(200)}_{disp}$: $E^{(200)}_{ind\_resp}$ –0.90 (0.86) for CdZn, 0.80 (0.82) for HgZn and 0.64 (0.58) for HgCd in ST97 (CRENBL) basis set. The higher orders of dispersion energies con-

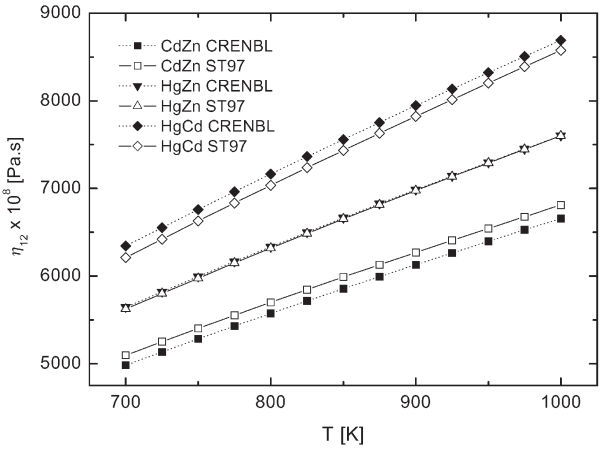

FIG. 3

Theoretical viscosities η_{12} for gas-phase IIB group elements. Full symbols are obtained using the CRENBL and open symbols using the ST97 basis set: CdZn (■, □), HgZn (▼, △) and HgCd (◆, ◇), respectively.

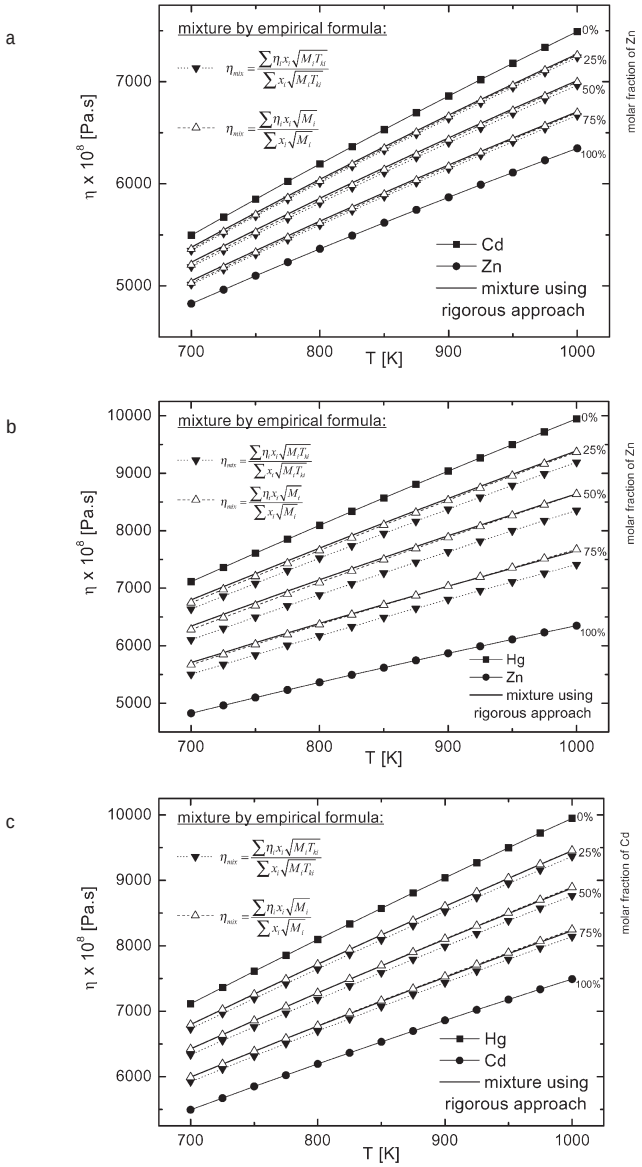

FIG. 4

Theoretical shear viscosities (from ST97 basis set potential curves) of pure gas-phase IIB group elements and their binary mixtures of 25, 50 and 75 mole % compositions for the mixtures of: a cadmium (■) and zinc (●), b mercury (■) and zinc (●), c mercury (■) and cadmium (●). Solid lines without symbols stand for the rigorous approach viscosities, dashed lines with symbols △ and ▼ stand for the viscosities obtained using empirical formulae (*16*) and (*17*), respectively

tribute minimally to the $E_{disp}^{(2)}$ ($E_{disp}^{(2)} = E_{disp}^{(200)} + E_{disp}^{(12)} + E_{disp}^{(22)}$) dispersion energy. These energies have a small stabilizing effect in the case of CdZn and HgZn dimers and almost no effect in HgCd. The electrostatic correlation energies are positive and little sensitive to the type of atoms involved in the interaction. The sum of the SAPT correlation contributions $E_{corr\_resp}^{SAPT}$ as calculated by SAPT 2003 is approximately 40% larger in magnitude than $\Delta E_{corr}^{CCSD(T)}$ for each system in both basis sets. Finally, in contrast to the ΔE^{SCF} energies, the repulsive $E_{exch\text{-}disp}^{(200)}$ and electrostatic correlation contributions ($E_{els\_resp}^{(12)} = E_{els\_resp}^{(120)} + E_{els\_resp}^{(102)}$)[23] do not significantly compensate the attractive dispersion energies.

In the next step the calculated potential energy curves were utilized to obtain temperature dependences of low-density shear viscosities. The results for η_{12} are depicted in Fig. 3. One can see a small discrepancy in CRENBL and ST97 results for CdZn and HgCd dimers and almost complete matching for the HgZn complex. The dependences of η_{12} on temperature are linear in the investigated temperature intervals. A comparison of theoretical and experimental low-density shear viscosity of pure IIB group elements was presented in our previous work[16]. Comparison of empirical formulae with a rigorous approach to shear viscosity calculation is depicted in Figs 4a–4c. From these figures it is clear that the empirical formula (*16*) without critical temperature involved provides better results for the viscosity of binary mixture composed of IIB group elements than the formula (*17*)

TABLE II
Experimental viscosities of the one-component IIB group gases and their binary mixtures

Component		*T*, K	Experimental viscosity (10^{-8} Pa s) for various % of component 1				
1	2		0	25	50	75	100
Cd	Zn	700	5 024	5 090	5 147	5 198	5 242
		1 000	6 854	7 003	7 132	7 245	7 344
Hg	Zn	700	5 024	5 712	6 212	6 593	6 891
		1 000	6 854	8 029	8 884	8 533	10 042
Hg	Cd	700	5 242	5 750	6 185	6 562	6 891
		1 000	7 344	8 175	8 887	9 504	10 042

of Herning and Zipperer which does involve the critical temperature. Therefore the formula not involving the critical temperature was used for calculations shear viscosities of the experimental binary mixtures from pure gases viscosities (Table II). The rigorously calculated shear viscosities of binary mixtures and their relative deviations from the experimental ones are summarized in Table III.

TABLE III
Rigorously calculated shear viscosities of binary mixtures and relative deviations from the experimental shear viscosities (calculated using formulae (*16*) and (*18*)–(*20*)) of Cd + Zn, Hg + Zn and Hg + Cd binary mixtures

Component		*T*, K	Rigorous approach viscosity (10^{-8} Pa s) and relative deviation (%) for various % of component 1					
1	2		25		50		75	
Cd	Zn	700	5 050	–0.8	5 232	+1.6	5 379	+3.5
		1 000	6 706	–4.2	7 012	–1.7	7 272	+0.4
Hg	Zn	700	5 707	–0.1	6 344	+2.1	6 798	+3.1
		1 000	7 651	–4.7	8 642	–2.7	9 389	–1.5
Hg	Cd	700	5 993	+4.2	6 425	+3.9	6 797	+3.6
		1 000	8 230	+0.7	8 880	–0.1	9 450	–0.6

CONCLUSION

The *ab initio* potential energy curves based on the pseudopotentials for heteronuclear IIB group diatomic complexes were evaluated at the supermolecular CCSD(T) level. The obtained potential energy curves can be well fitted by the Morse potential function. In the minima of potential energy curves the interaction energy was separated into fundamental components using the I-PT. The importance of the dispersion interaction in comparison with the induction interaction increases with increasing internuclear separation, i.e. it has the highest value for the CdZn complex and the lowest one for the HgCd complex. The Morse fit of the potential curves presented in this work as well as the potential curves of homonuclear systems from our previous work[16] was used to simulate the temperature dependences of low-density shear viscosity of binary mixtures. In addition to the rigorous kinetic theory approach, empirical formulae for

binary mixture viscosity were applied. The agreement between the rigorous approach and the empirical formulae usually used in technical practice is fairly good.

There is a wide variability of equilibrium interatomic distances in different theoretical and experimental studies. Possibly the experimental shear viscosities of binary mixtures of group IIB element, or, better, diffusion coefficients, which are closely related to η_{12} viscosities and are dependent only on heteronuclear potential energy curves, can offer a clue to the correct values of equilibrium distances.

The work has been supported by the Slovak Grant Agency (Projects Nos 1/3566/06 and 1/2021/05).

REFERENCES

1. Krause L., Kedzierski W., Czajkowski A., Atkinson J. B.: *Phys. Scr.* **1997**, *T72*, 48.
2. Macrae V. A., Greene T. M., Downs A. J.: *J. Phys. Chem. A* **2004**, *108*, 1393.
3. a) Hegazi E., Supronowicz J., Atkinson J. B., Krause L.: *Phys. Rev. A* **1990**, *42*, 2734; b) Supronowicz J., Hegazi E., Atkinson J. B., Krause L.: *Chem. Phys Lett.* **1994**, *218*, 240; c) Supronowicz J., Hegazi E., Atkinson J. B., Krause L.: *Chem. Phys Lett.* **1994**, *222*, 149.
4. Braune H.: *Z. Phys. Chem.* **1928**, *137*, 447.
5. Ceccherini S., Morraldi M.: *Chem. Phys. Lett.* **2001**, *337*, 386.
6. a) Czajkowski M. A., Koperski J.: *Spectrochim. Acta, Part A* **1999**, *55*, 2221; b) Koperski J., Atkinson J. B., Krause L.: *Can. J. Phys.* **1994**, *72*, 1070.
7. Dolg M., Flad H. J.: *J. Phys. Chem.* **1996**, *100*, 6147.
8. Munro L. J., Johnson J. K., Jordan K. D.: *J. Chem. Phys.* **2001**, *114*, 5545.
9. Bieroń J. R., Baylis W. E.: *Chem. Phys.* **1995**, *197*, 129.
10. Schwerdtfeger P., Wesendrup R., Moyano G. E., Sadlej A. J., Greif J., Hensel F.: *J. Chem. Phys.* **2001**, *115*, 7401.
11. Peterson K. A., Puzzarini C.: *Theor. Chem. Acc.* **2005**, *114*, 283.
12. Czuchaj E., Rebentrost F., Stoll H., Preuss H.: *Chem. Phys. Lett.* **1996**, *255*, 203.
13. Czuchaj E., Rebentrost F., Stoll H., Preuss H.: *Chem. Phys. Lett.* **1994**, *225*, 233.
14. Ellingsen K., Saue T., Pouchan C., Gropen O.: *Chem. Phys.* **2005**, *311*, 35.
15. Yu M., Dolg M.: *Chem. Phys. Lett.* **1997**, *273*, 329.
16. Lukeš V., Ilčin M., Laurinc V., Biskupič S.: *Chem. Phys. Lett.* **2006**, *424*, 199.
17. Czuchaj E., Rebentrost F., Stoll H., Preuss H.: *Chem. Phys. Lett.* **1992**, *197*, 187.
18. Czuchaj E., Rebentrost F., Stoll H., Preuss H.: *Chem. Phys. Lett.* **1993**, *212*, 534.
19. Gao F., Yang C.-L., Ren T.-Q.: *J. Mol. Struct. (THEOCHEM)* **2006**, *758*, 81.
20. Bieroń J., Baylis W. E.: *Mol. Phys.* **2000**, *98*, 1051.
21. a) Supronowicz J., Petro D., Atkinson J. B., Krause L.: *Phys. Rev. A* **1994**, *50*, 2161; b) Supronowicz J., Atkinson J. B., Krause L.: *Phys. Rev. A* **1994**, *50*, 3719.
22. Supronowicz J., Kedzierski W., Atkinson J. B., Krause L.: *Phys. Rev. A* **1992**, *45*, 538.
23. Jeziorski B., Moszyński R., Ratkiewicz A., Rybak S., Szalewicz K., Williams H. L. in: *Methods and Techniques in Computational Chemistry: METECC-94* (E. Clementi, Ed.), Vol. B. STEF, Cagliari 1993.

24. Chałasiński G., Szczęśniak M. M.: *Chem. Rev.* **1994**, *94*, 1723.
25. a) Kvasnička V., Laurinc V., Biskupič S.: *Mol. Phys.* **1980**, *39*, 143; b) Kvasnička V., Laurinc V., Biskupič S.: *Czech. J. Phys. B* **1981**, *31*, 41.
26. Kvasnička V., Laurinc V., Biskupič S.: *Phys. Rep.* **1982**, *90*, 159; and references therein.
27. Löwdin P.-O.: *Adv. Phys.* **1956**, *5*, 1.
28. Lukeš V., Laurinc V., Biskupič S.: *Int. J. Quantum Chem.* **1999**, *75*, 81; and references therein.
29. Lukeš V., Laurinc V., Biskupič S.: *J. Comput. Chem.* **1999**, *20*, 857.
30. Kochanski E.: *J. Chem. Phys.* **1973**, *58*, 5823.
31. Maitland G. C., Rigby M., Smith E. B., Wakeham W. A.: *Intermolecular Forces*. Clarrendon Press, Oxford 1981.
32. Hirschfelder J. O., Curtiss Ch. F., Bird R. B.: *Molecular Theory of Gases and Liquids*. John Wiley & Sons, New York 1954.
33. Frisch M. J., Trucks G. W., Schlegel H. B., Scuseria G. E., Robb M. A., Cheeseman J. R., Montgomery J. A., Jr., Vreven T., Kudin K. N., Burant J. C., Millam J. M., Iyengar S. S., Tomasi J., Barone V., Mennucci B., Cossi M., Scalmani G., Rega N., Petersson G. A., Nakatsuji H., Hada M., Ehara M., Toyota K., Fukuda R., Hasegawa J., Ishida M., Nakajima T., Honda Y., Kitao O., Nakai H., Klene M., Li X., Knox J. E., Hratchian H. P., Cross J. B., Adamo C., Jaramillo J., Gomperts R., Gonzalez C., Pople J. A.: *Gaussian 03,* C.02. Gaussian, Inc., Pittsburgh (PA) 2003.
34. Boys S. F., Bernardi F.: *Mol. Phys.* **1970**, *19*, 553.
35. Küchle W., Dolg M., Stoll H., Preuss H.: *Mol. Phys.* **1991**, *74*, 1245.
36. a) LaJohn L. A., Christiansen P. A., Ross R. B., Atashroo T., Ermler W. C.: *J. Chem. Phys.* **1987**, *87*, 2812; b) Ross R. B., Powers J. M., Atashroo T., Ermler W. C., LaJohn L. A., Christiansen P. A.: *J. Chem. Phys.* **1990**, *93*, 6654.
37. Tao F.-M., Pan Y.-K.: *J. Chem. Phys.* **1992**, *97*, 4989.
38. Baker J. A., Fock W., Smith F.: *Phys. Fluids* **1964**, *7*, 879.
39. Herning F., Zipperer L.: *Gas Wasserfach* **1936**, *79*, 69.
40. Mc Geoch M. W., Fournier G. R., Ewart P.: *J. Phys. B* **1976**, *9*, L121.